Nuclear Instruments and Methods in Physics Research A 349 (1994) 438–446
North-Holland

NUCLEAR INSTRUMENTS & METHODS IN PHYSICS RESEARCH
Section A

Study of inclined particle tracks in micro strip gas counters

F.D. v.d. Berg [a], F.G. Hartjes [a,*], J. Schmitz [a], F. Udo [a], A.R. de Winter [a], B. Dutrieue [b], C. Vander Velde [b]

[a] *NIKHEF-H, Amsterdam, The Netherlands*
[b] *IIHE-ULB, Brussels, Belgium*

Received 16 February 1994; revised 11 May 1994

The response of micro strip gas counters (MSGC) has been studied for particle tracks with inclined incidence with respect to the strip plane. The setup consisted of four 10×10 cm^2 MSGC detectors arranged in a cosmic ray hodoscope with a trigger threshold of 300 MeV/c for muons. Results are given for the collected charge, the spatial resolution and the detection efficiencies. A Monte Carlo simulation has been used to understand the effects of cross talk in the data and to extrapolate the data to other angles of incidence.

1. Introduction

Since their introduction in 1988 [1], micro strip gas counters (MSGC) have been tested by several groups and their qualities were demonstrated in many respects: a position accuracy as good as 30 μm with a detection efficiency of 96% for minimum ionizing particles [2,3], a rate capability above 5×10^5 mm^{-2} s^{-1} for irradiations with 9 GeV photons from an X-ray tube [4] and an energy resolution of 11% FWHM for the ^{55}Fe 5.9 keV X-ray peak, obtained with proportional gains up to 10^4 [5].

The spatial resolution and efficiency quoted above were obtained for particles travelling perpendicular to the micro-strip plane. The situation changes if the polar angle θ is different from zero as illustrated in Fig. 1: the electrons left by the particle spread over many strips. The charge collected by each strip is proportional to the ionization in the gas column above the strip. The extreme case is given by a particle travelling parallel to the strip plane, perpendicular to the strips. The particle path length in this column is then given by the anode strip separation which is typically 200 μm. In this case the probability to have no ionization at all above a strip is thus high, leading to large inefficiencies per strip. The strip efficiency for such tracks was measured to be as low as 6%, in the same experimental conditions which produce a 96% track efficiency for orthogonally incident particles [3]. This is considered as an advantage for a tracking detector at a future proton collider [6], as the particles with a low transverse momentum, trapped in a magnetic field of several Tesla, would remain partially undetected, reducing the occupancy of the detector. However, it should be checked that at intermediate angles, the strip efficiency and the resolution remain sufficient to be able to reconstruct the track of particles with transverse momenta down to 5 GeV/c, as required by the physics goals of the experiments [7,8]. Some physics studies like the search for CP violation effects in the B system, through the channel: B_d^0, $\overline{B_d^0} \rightarrow J/\Psi K^0 \rightarrow \mu^+\mu^-\pi^+\pi^-$, would even benefit from a lower p_T detection in order to reach an efficient reconstruction of the K^0 decay [9].

This paper presents an experimental study of the response of MSGC counters to cosmic ray particles travelling in a plane perpendicular to the strips, with polar angles between 0° and 51°. The results show several unexpected features, so it was felt necessary to adapt an existing Monte Carlo program [10] to this setup to verify our understanding of the results. Sections 2, 3 and 4 present the experimental setup and explain the data analysis. Section 5 introduces the Monte Carlo program and Section 6 discusses the experimental results and demonstrates the agreement between MC and data. Section 7 presents an analysis of the detector based on simulated data and a prediction of the response of the MSGC to incident angles not measured in the present experiment.

2. The experimental setup

The MSGC detectors used are made of 300 μm thick borosilicate glass substrates [11], 10×10 cm^2, carrying 500 aluminium anode–cathode pairs, 1 μm thick. The widths of the electrodes are 7 μm and 90 μm for anodes and cathodes respectively, with a 200 μm pitch between two successive anodes. The drift electrode is situated on a 200 μm thick borosilicate glass plate, 3 mm above the

* Corresponding author. Tel.: +31 (20) 592 5010; Fax: +31 (20) 592 5155.

SSDI 0168-9002(94)00629-L

strip plane. Four such detectors are placed horizontally 12.7 mm above each other, with their strips running parallel. The stack is placed in a gas tight box in which a 60–40% DME/CO_2 gas mixture is flushed. The layers are numbered 1 to 4 from top to bottom.

The anode strips are grounded while the cathode strips, grouped in units of sixteen, are put to a voltage of -620 V. The drift electrode is at -2500 V resulting in a maximum drift time of about 60 ns. The gas gain is between 1000 and 2000, leading to an input signal of about 60 000 electrons for tracks perpendicular to the detector plane. The anode signals are read out with preamplifiers packed in MX5 chips [12]. These chips each contain 128 channels and a serial readout system. Their frontends have a slow integrator preamplifier circuit set at 600 ns rise time. The readout method is a double correlated sampling, of which the first sample serves as reference. A trigger signal is required to initialize the readout. In the present setup, it is provided by a scintillator coincidence and as it arrives with a delay of 120 ns, it causes an average signal loss of about 30%. The input noise is less than 1000 electrons. The digitising of the 500 signals of one layer of detection is done serially into a Sirocco flash ADC unit operating at 1.2 MHz [13]. This unit performs automatic pedestal subtraction and zero suppressing.

Cosmic ray particles travelling in a plane approximately perpendicular to the strips are selected by means of a triple scintillator coincidence. The widths of the scintillators and their relative distances insure that the polar angle of the track, projected in a vertical plane parallel to the strips, φ, is less than 17° (see Fig. 2a). The MSGC stack height and the position of the central scintillator limit the polar angle of the track, projected in the plane perpendicular to the strips, θ, to a maximum value of 51° (see Fig. 2b). With the restriction of φ smaller than 17°, the particle path length in the gas column above a given strip is fixed by the value of θ to within $\pm 4\%$. An absorber made of 8 cm of iron and 3 cm of lead, placed above the lower scintillator, insures the selection of muons with a momentum above 300 MeV/c.

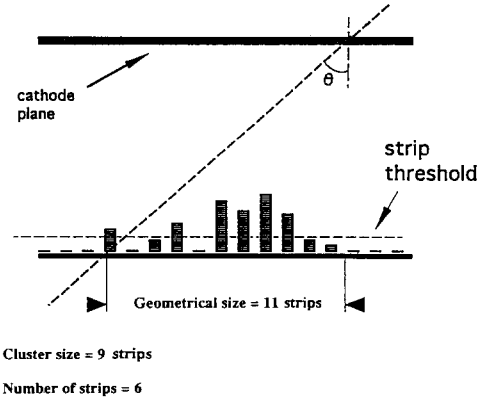

Fig. 1. Schematic cross section of a MSGC showing the charges produced on several anode strips by a particle at non normal incidence.

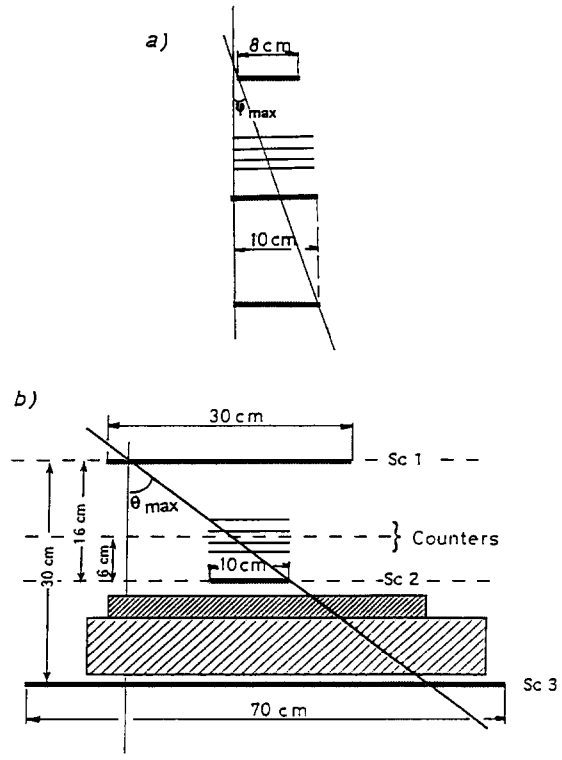

Fig. 2. Vertical cross sections of the experimental set up, showing four MSGC's, the trigger scintillators, SC1, SC2 and SC3 and the absorbers of lead and iron (hatched), in a plane parallel to the strip electrodes (a) and in a plane perpendicular to them (b).

All scintillator triggers giving rise to at least three detector layers with an anode signal above threshold are written onto disk. The threshold is equal to 10 ADC counts. One electron corresponds approximately to 7 to 12 ADC counts depending on the layer.

Higher threshold values are used in the off-line analysis. These values are 20, 15 and 18 ADC counts for layers 1, 2 and 4 respectively. They are adjusted taking into account the detector efficiency and the occurrence of noisy channels. The threshold in layer 3 is taken to be 20, but for some data the behaviour as a function of threshold is presented.

Observing the distributions of the number of hits on each strip allows to detect the noisy and weak channels and to remove them from the subsequent analysis. A channel is declared noisy, if it counts approximately three times more than the average. Depending on the runs, about 40 such channels are detected on a total of 2000 strips, mostly in layer 4. Layer 3 has the smallest number of noisy channels and for this reason all data quoted in this paper are from plane 3 for tracks defined in the layers 1,2

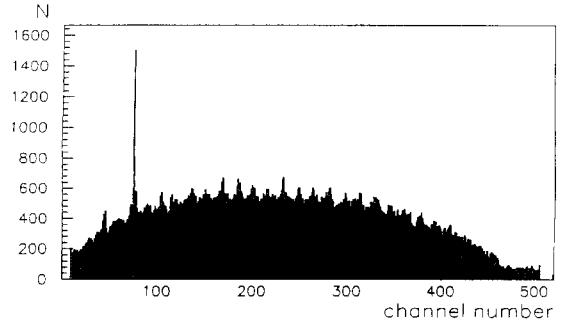

Fig. 3. Distribution of hits per anode channel for the third MSGC.

and 4. Fig. 3 shows the hit distribution in layer 3. The oscillations observed with a period of sixteen channels result from the connection of the cathodes in groups of sixteen. As a result the impedance of the anode circuit changes on the border of two cathode blocks, so its signal is slightly larger than that of the others. To avoid the influence of edge effects deforming the electromagnetic field distribution, strips numbered below 41 and above 465 are not used in the analysis.

3. Detector alignment

At first, the four detectors were aligned parallel to each other, with an accuracy of ± 150 μrad.

The relative displacement of the detectors is measured using clean vertical tracks, selected by requiring events with at most one or two contiguous hits per layer and at least three layers hit. The positions of the clusters, p_i, are determined in each layer i from the centre of gravity of the signal charges. The events are then kept only if the reconstructed positions are compatible with the hypothesis of a single straight track. This check is done using the following variables:

$$t_1 = (p_2 + p_4)/2 - p_3,$$

$$t_2 = (p_1 + 2p_4)/3 - p_3,$$

$$t_3 = (2p_1 + p_4)/3 - p_2,$$

$$t_4 = (p_1 + p_3)/2 - p_2.$$

When it is possible to calculate one of these variables, it has to be in agreement with the mean value of its distribution, within two standard deviations.

For the accepted events, the distributions of the position differences in various layers, $p_i - p_j$, are studied. As care is taken to select events with a θ distribution symmetric around zero, non-zero average values for the position difference distributions have to be attributed to misalignments. Following this analysis using between 7000 and 10000 events, the strips have to be shifted by (-109 ± 18) μm, (362 ± 9) μm, 0. and (-494 ± 9) μm for layers 1 to 4 respectively, with an additional systematic error of 20 μm due to possible small angular asymmetries in the event selection.

With the above first analysis the vertical direction is known to better than 0.2°, which is more than sufficient to study angular effects in MSGCs. However, the imprecision of more than 20 μm on the individual strip position could contribute significantly to the estimated position resolution. For this reason a second iteration of the alignment is performed by fitting straight lines to the positions p_i, using the minimum χ^2 method. Non zero means for the distributions of the residuals are attributed to misalignment. The resulting shifts are now: $(-107.9 \pm .4)$ μm, $(376.2 \pm .4)$ μm, 0. and $(-530.0 \pm .4)$ μm. Applying directly this second method would give a wrong estimation of the vertical direction, by about two degrees.

To check also the parallelism of the detectors, a special run was taken: the scintillators were displaced in order to select particles hitting preferentially one end of the strips. No effect is observed on the layer shifts within a precision of 5 μm.

4. Cluster and track definitions for large angle studies

In order to study parameters like the strip efficiency and the spatial resolution, clean isolated tracks are defined using only layers 1, 2 and 4. A track is accepted if a single cluster of hits is found in each of the three layers and if their positions are in agreement with the hypothesis of a straight track. For this track definition the cluster position is defined by the centre of gravity method. The alignment of the three clusters is checked using the variable t_3, defined in Section 3. However here the half road width on $|t_3|$ is adapted to the angle of incidence of the track. It is taken to be: $220 + 1000\ |\tan\theta|$ (μm). This choice of the angular dependence of the road width does not impair the efficiency of the track finding.

For a track with $\theta = 36°$, as on Fig. 1, the particle passes over eleven strips; this number is called the geometrical size of the cluster associated to this track angle. As pointed out in the introduction, the strip efficiency rapidly decreases with the polar angle θ. As a result many of these eleven strips might give no signal above threshold leading to several consecutive zeros between two detected hits. In order to include all detected hits in the cluster definition it is necesserary to allow up to ten consecutive zeros in the cluster definition. The cluster size is then defined as the number of strips from the first to the last detected strips; generally it will be smaller than the geometrical cluster size, due to the strip inefficiencies, but not always: it may be larger due to the diffusion of the primary electron swarm during the drift. The number of strips, defined as the number of strips with a signal above threshold within the cluster, is also generally smaller than the cluster size due to the strip inefficiencies.

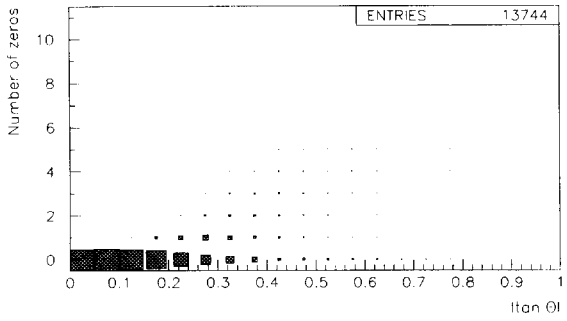

Fig. 4. Distribution of the number of strips with no charge above threshold within a cluster as a function of $|\tan\theta|$.

The cluster definition described above serves to find all strips hit, but it is only applicable in case of a low track multiplicity, in a low noise environment. Allowing ten consecutive zeros is rarely possible in a real experiment as the occupancy with real and background tracks prevents this. At best one strip without charge can be allowed, but even that might spoil the two track resolution. In addition, it is also unnecessary to allow for many zeros if the interesting tracks impinge nearly vertically on the detector. This can be observed in Fig. 4, showing the total number of zeros in a cluster as a function of the track slope. At incidence angles smaller than 5.7° from the normal, only $(0.3 \pm 0.1)\%$ of the tracks produce a cluster with missing hits. This number increases to $(2.2 \pm .4)\%$ between 5.7° and 8.5°, and $(12.0 \pm 0.8)\%$ between 8.5° and 11.3°. Allowing a single zero maintains this fraction below 0.5% up to 12°.

For the accepted events, the cluster positions, p_1, p_2 and p_4, are fitted to a straight line, by the minimum χ^2 method. The distribution of the polar angle θ for the selected tracks is peaked at 0° (vertical tracks) falling to zero at 51°. With a signal threshold of 20 ADC counts, corresponding to about three primary electrons, the data are very clean: only 1.4% of the events have more than one cluster per plane.

The expected coordinate of the track impact point in layer 3, x_3, is calculated from the fitted track parameters. It is then compared to the measured cluster positions in layer 3. The nearest cluster in layer 3 is attributed to the track only if: $|x_3 - p_3| < 300 + 1800\,|\tan\theta|$ (μm). This limit is well above the dispersion of the data, which are presented in Section 6.

5. Monte Carlo simulations

To better understand the experimental results a Monte Carlo (MC) program, developed in 1991 [10], was adapted to simulate the experimental set up. The original program simulates the response of MSGCs, taking into account primary and secondary ionizations, the drift and transverse diffusion of electrons and the average gas gain with its fluctuations. A cosmic ray generator taking into account the present experimental conditions was added to the original program to simulate tracks in the four detectors with the correct angular and position distribution. It includes the simulation of multiple scattering and energy losses in the material of the set up and in the four ceilings of concrete above it. The geometrical acceptance of the scintillators and the detectors is also incorporated. The detectors are supposed to be parallel, but with the same shift in the relative position of the strips as in the real data.

With this program the signals are calculated in the four MSGC layers under the assumption, that the cosmics have identical energy loss behaviour (so the momentum of the particles is assumed fixed). The signal loss in the MX5 preamplifiers resulting from the delay of the trigger pulse is taken into account. No dead or noisy channels are generated in the Monte Carlo, but the program creates an output file in the same format as the data acquisition software, so that one analysis program has been used to interpret both information streams. This implies, that all noisy and dead channels present in the experiment are also treated as such in the MC data.

Some free parameters in the simulation had to be tuned: the transverse diffusion coefficient and the relation between the number of liberated electrons and the eventual output signal in ADC counts for each layer. Each anode strip on one layer is assigned the same gas amplification factor. The relation fitted for layer 3 is 7 ADC counts per electron. Note that with the threshold at 10 ADC counts, the setup is almost single-electron sensitive despite the gas amplification of only 1000. The transverse diffusion coefficient is found to be 64 $\mu m/\sqrt{cm}$, well in agreement with earlier measurements at different settings of the high voltage.

It was necessary to distinguish between the electrons liberated in the drift field and those from the quadrupole region directly above the strips. The latter can undergo a much higher amplification because they do not follow the regular drift lines towards the anodes. When the angle of incidence is high, this effect can be seen as the average signal on one side of the cluster being higher than on the other side. As a rough approximation all electrons liberated in the quadrupole field are assigned a gas amplification twice as high as the others. This factor 2 was established from the requirement to get a good correspondence between the data and MC for this particular phenomenon. For a better approximation one needs knowledge of the electric field in the quadrupole region and the first Townsend coefficient over a wide range of E.

The main uncertainties that limit the predictive power of the MC are the effect of the energy spectrum of the cosmic ray muons, the variation in the momentum distribution as a function of θ, and the primary and secondary ionization process. These three processes each contribute

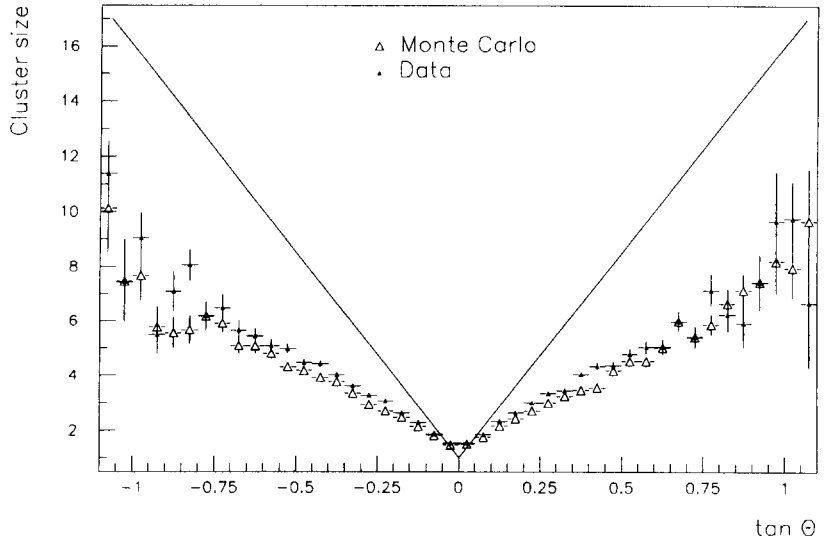

Fig. 5. Average cluster size as a function of the track slope for data and simulated data. The clustersize is defined as the distance from the first to the last strip with a signal above 20 ADC counts in a cluster as explained in Fig. 1. Up to 10 zeros are allowed between signals in a cluster.

around 5% to the total error on critical observables like the average cluster size.

6. Results

Fig. 5 shows the average cluster size as a function of the track slope both for experimental and MC data. The line represents the relation expected for the cluster size proportional to the track projection at any angle. It is observed that for all but the lowest angles ($|\tan\theta| > 0.05$), the average cluster size is well below the expected value, due to the strip inefficiencies. It is above the expected value at perpendicular incidence due to diffusion. The tails of the cluster size distribution (not shown) reach just to the geometrical limit for all but the largest angles. Fig. 6 shows the angular dependence of the average number of strips hit within a cluster again for the data and MC results. It is never above four at any angle, demonstrating the necessity to allow for zeros between detected strips if

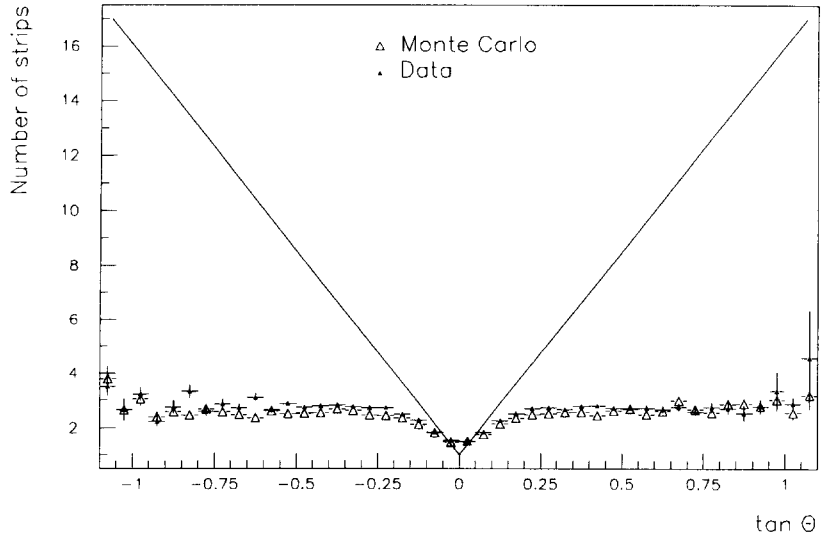

Fig. 6. Average number of strips with a signal above threshold within the clusters as a function of the slope of the track for the same data as displayed in Fig. 5.

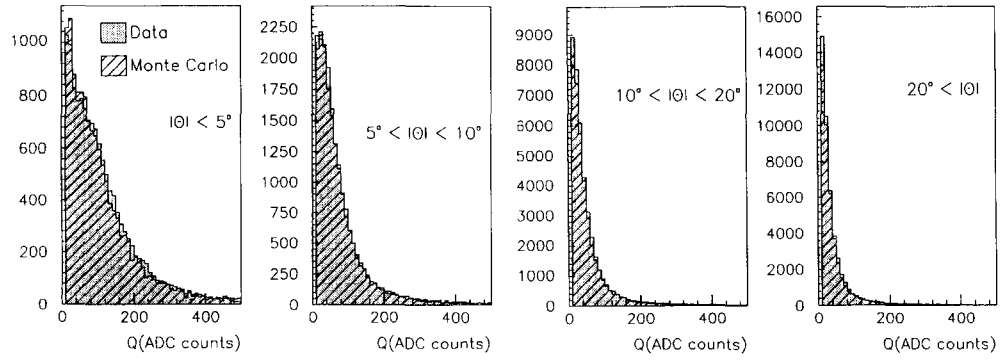

Fig. 7. Distributions of the strip charge in four ranges of the track slope.

the cluster size has to be determined correctly and the number of clusters per layer not to be increased artificially. The data are above the MC results by a fraction of a strip in both Figs. 5 and 6. The agreement between data and MC results does not change if the number of zeros allowed in a cluster is lowered to one. This demonstrates, that the high number of accepted zeros between two detected hits rarely associates random hits to a cluster, as the MC data do not contain random hits. This is achieved thanks to the low noise rate of the detectors and the low track multiplicity in cosmic data.

Not only the number of detected strips is affected by the particle incidence angle, but also the charge collected by each strip. Fig. 7 shows the distribution of this charge for data and MC, for four angular regions. At small angles, the average charge decreases rapidly as the angle increases: it is already reduced by a factor two from $|\theta| < 5°$ to $|\theta| = 15°$. The figure shows, that the simulated data follow the measured pulse height distributions quite accurately. The behaviour of the charge per strip implies that increasing the threshold influences strongly the number of hits in a cluster at large angles, but the efficiency at normal incidence is hardly affected.

Contrary to expectations, the total cluster charge does not increase with angle despite the fact that the effective path of the particle in the gas is inversely proportional to $\cos\theta$. This effect is dependent on the strip threshold. Fig. 8 shows the angular dependence of the measured cluster charges for two strip thresholds, 10 and 20 ADC counts. Simulated data are only given for the lowest threshold. Two effects contribute to the lack of charge at large angles. First, many strip signals remain below threshold at large angles and do not contribute to the cluster charge calculation. Second, the cathode strips are connected in groups of sixteen, without further capacitive decoupling. This causes a negative feedback of 6% between an anode with a signal and its fifteen neighbours. In the limit of a homogeneous charge distribution no charge would be detected at all. This effect tends to suppress large size clusters. The simulation data are 15% above the experimental results, although Fig. 7 shows, that the pulse height distributions are quite well reproduced by the calculation.

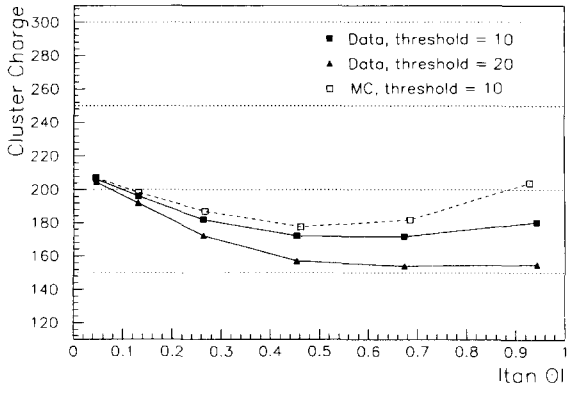

Fig. 8. Angular distribution of the average charge per cluster for two signal thresholds. The MC result is shown only for a threshold of 10.

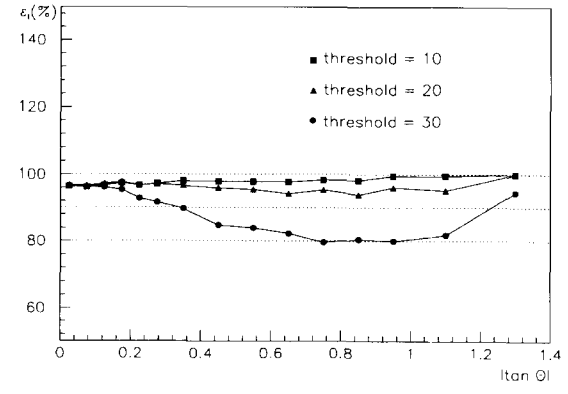

Fig. 9. Measured efficiency of the third detector ε_L as a function of the track slope, for various strip thresholds given in ADC counts.

The detection efficiency of layer 3, ε_L is easily deduced from the fraction of fitted tracks that have at least one cluster in layer 3 with a measured position in agreement with the fit prediction (see Section 4). No restriction is applied on the total number of clusters observed in layer 3. Fig. 9 shows the layer efficiency ε_L as a function of the track slope $|\tan\theta|$, for various values of the signal threshold. It is seen that it remains above 90% at any angle, provided that the signal threshold is kept sufficiently low, of the order of 20 ADC counts. It should be noted that the cluster may be reduced to a single detected hit even at large angles. This explains why the layer efficiency is much higher than the single strip efficiency that is estimated in the next paragraph and why it increases at the largest angles, with the number of strips likely to give a signal.

The strip efficiency, ε_s, is defined as the average probability for one strip, to give a signal above threshold when a minimum ionizing particle traverses the gas column spanned by that strip. For a given polar angle range, it is measured as the total number of strips observed with a signal above threshold, divided by the total number of strips that should have fired. This last number is given by the geometrical cluster size, deduced from θ (see Fig. 1), increased by a constant term d, that takes into account the diffusion and a geometrical effect: a track with $|\theta| < 3.81°$, with a geometrical size of one, can leave half of its primary ionization over one strip and half of it over the neighbouring strip. Taking into account the layer efficiency and the observed hit multiplicity at small angles, we assume $d = 0.68$ in units of one strip, with a systematic error of 0.05 leading to an error on ε_s of less than 3% for perpendicular tracks, and negligible at large angles.

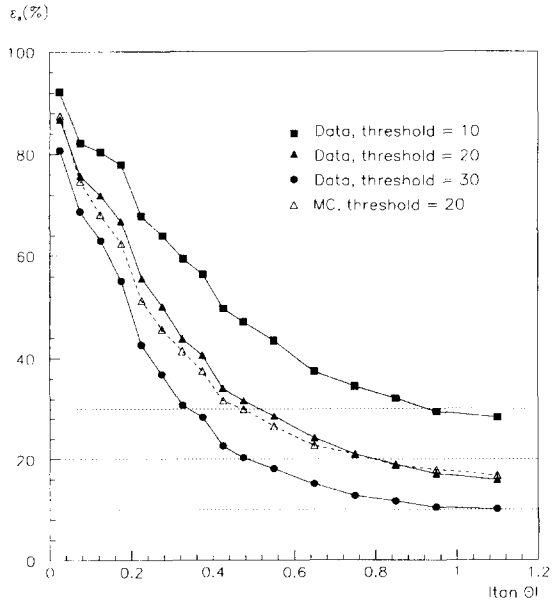

Fig. 10. Average strip efficiency in a cluster ε_S as a function of the track slope for three thresholds (in ADC counts). The dotted line is the calculated curve for a threshold of 20.

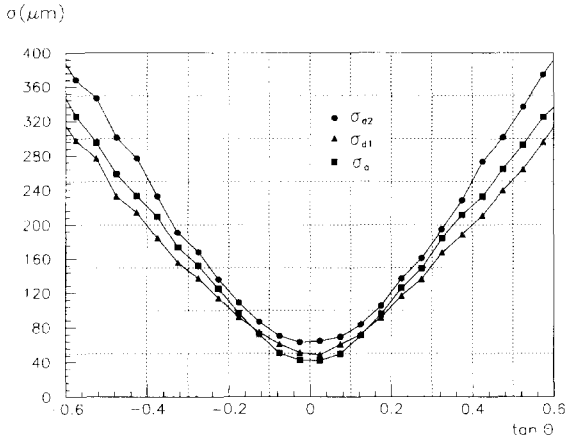

Fig. 11. Spatial resolution as a function of the track slope for three different methods of defining a a cluster position: the centre of gravity of the charge (σ_a.), the average position of the first and last strip detected in the cluster (σ_{d1}), the position of the strip collecting the electrons with the shortest drift time (σ_{d2}).

The strip efficiency ε_s, is shown in Fig. 10 as a function of the track slope $|\tan\theta|$ for various values of the signal threshold. It is observed to drop rapidly with the angle, reaching less than 20% for angles larger than 40° and thresholds higher than 20 ADC counts. The dotted line is the curve predicted by the simulation for a threshold of 20 ADC counts. The figure shows, that the MC underestimates the efficiency for most of the angular range.

The spatial resolution is obtained from the average χ^2 per degree of freedom of a linear four points fit through the measured cluster positions. It is estimated for three different methods to define the cluster position. The centre of gravity method, used up to now, is called the analog method, and the corresponding resolution, σ_a. The two other methods do not use the charge values and are called digital methods; the corresponding resolutions are labelled σ_{d1} and σ_{d2}. For the first digital method the cluster position is taken as the average position of the first and last strips detected in the cluster. For the last method, the cluster position is attributed to the strip collecting the electrons with the shortest drift time, the first or the last one in the cluster depending on the sign of the polar angle. The residuals obtained in layer 3 have an average value of (3.0 ± 1.4) μm, (7.2 ± 1.3) μm and (8.0 ± 1.6) μm for the three different methods, respectively. The two last values show a small systematic effect due to the discrete definition of the position while the alignment is performed with the analog definition of the position. Fig. 11 shows these resolutions σ_a, σ_{d1} and σ_{d2}, measured with a threshold of 20 counts, as a function of tan θ. It should be mentioned, that these resolutions include a contribution

from multiple scatterings in the plates. Taking that effect into account the best resolution is smaller than 40 μm obtained for tracks perpendicular to the strip plane and using the analog method. What is surprising is that the first digital method is less than 10 μm worse than the analog method and this up to a deviation of 8° from perpendicular incidence only. At larger angles the resolution of the first digital method becomes even better than the analog one. The second digital method is definitely inferior to the other two at any angle but the increase in resolution is less than $\sqrt{2}$ as would be expected if the first and last strips suffered from the same spatial dispersion. The degradation of the resolution with the polar angle is rather fast: the best resolution reaches already 300 μm at 30° from normal incidence! At small angles ($< 12°$), the spatial resolution is almost not influenced by the threshold, at least for values not larger than 30 ADC counts. All these features of the resolution curves are well reproduced by the simulation. The MC underestimates the resolution by about 5 μm at normal incidence. This can be understood by the fact, that the reference counters were far from perfect, so the measured track contained errors due to these imperfections. At larger angles the agreement between measured and calculated values is better, because these effects are negligible there.

7. Monte Carlo predictions

The MC describes the data well enough to use it to determine the influence of the negative cross talk as discussed in Section 6. The effect on the pulse height per strip was already discussed in connection with the oscillations observed in the hit distribution presented in Fig. 3. The MC reproduces this effect exactly. To check the contribution of the cross talk to the suppression of the response at large angles, the program was run with the cross talk switched off. Fig. 12 shows the ratio between the strip efficiencies in the two cases. It shows, that the

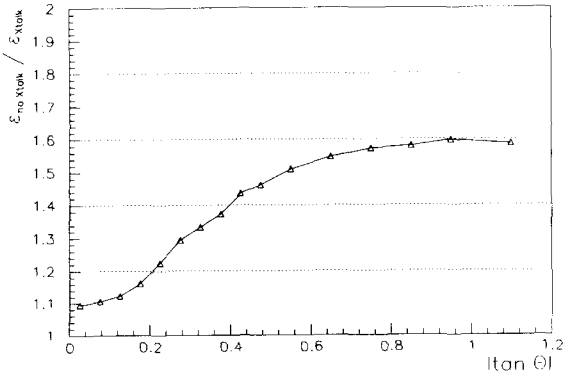

Fig. 12. Ratio of the calculated strip efficiencies ε_S without and with cross talk as a function of the track slope.

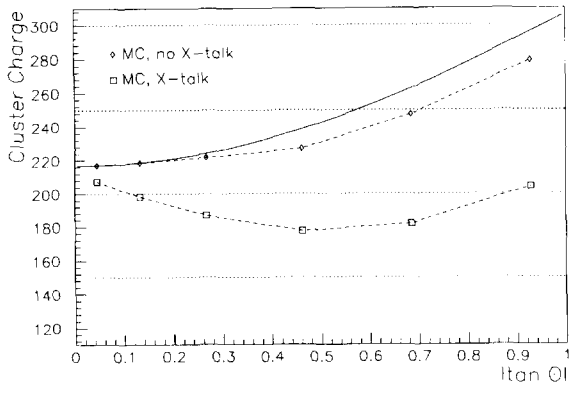

Fig. 13. Simulated angular dependence of the average cluster charge without and with cross talk. The solid line represents the relation according to the geometrical length of the track in the gas: $Q = Q_0 \cos \theta$.

cross talk reduces the number of hits at large angles by 60%. Fig. 13 shows, that the angular dependence of the total cluster charge without cross talk approaches closely the behaviour as expected from simple geometry, so the losses at large incident angles as observed in the data are mainly due to cross talk, provided that the threshold is only a few primary electrons equivalent.

Not surprisingly the resolution is better at large angles if no cross talk is present. The improvement becomes significant beyond $\tan \theta = 0.16$.

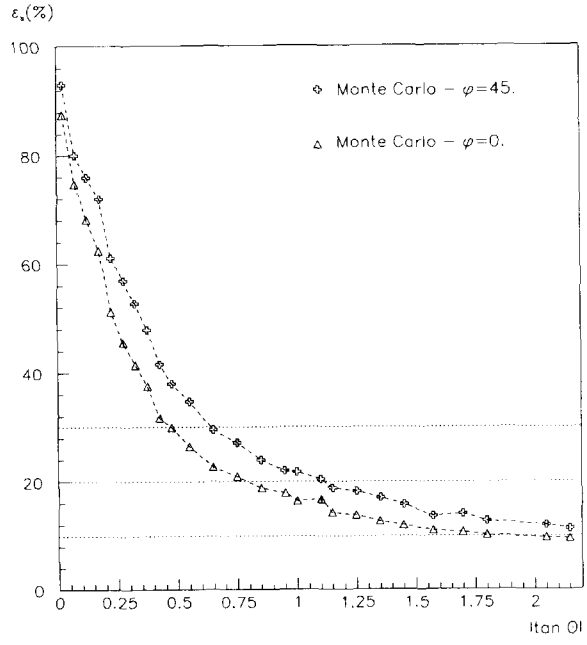

Fig. 14. Angular dependence of the calculated strip efficiency ε_S for two angles in phi: at $\varphi = 45°$ and at normal incidence as used in this experiment represented by $\varphi = 0°$.

Complementary to the non perpendicular incidence in θ as discussed here, one can study the effect of non perpendicularity in the other plane containing the vertical, as indicated by the angle phi as defined in Fig. 2a. The projected trackers at LHC [6] allow the angle phi to be anywhere from 0° to 45°, so here we present calculations in which the setup is rotated by 45° in phi. At this angle the ionization trail in the gas is longer by $\sqrt{2}$, so the effect will be an increase in pulse height and in strip efficiency at large angles. Fig. 14 illustrates this by comparing the strip efficiency in the two cases.
The conclusion is, that the strip efficiency is 30% better at phi = 45°. The resolution (not shown) is slightly better in the 45° case. The cross talk was switched on again in these runs.

8. Conclusions

The present experiment confirms that the strip efficiency of MSGCs decreases rapidly as the polar angle θ, in the plane perpendicular to the strips, increases. In the present construction of the detectors, it falls below 30% or even 20% for $\theta \geq 30°$, depending on the signal threshold. The influence of the cross talk on this effect is demonstrated via an MC calculation. However, if required, large layer detection efficiencies, above 90%, can be maintained at all angles, by using a signal threshold, corresponding to about two primary electrons. As expected the spatial resolution degrades also with the polar angle going from about 40 μm for perpendicular tracks to about 300 μm at 30°. It is also shown that in practical applications the spatial resolution is not an important argument to choose between analog or digital readout as both methods lead to resolutions that are not different by more than 10 μm at perpendicar incidence. These resolutions are hardly affected by the threshold values adopted, especially at angles lower than about 12°. In a LHC environment, this should allow to tune the threshold in order to keep a high track reconstruction efficiency at small angles while a large fraction of the hits produced by looping tracks are not detected. The change in response to tracks inclined in a plane containing the strips has been calculated and is shown not to be very different from the response as measured in this experiment.

References

[1] A. Oed, Nucl. Instr. and Meth. A 263 (1988) 351.
[2] F. Angelini et al., Nucl. Phys. 23 A (1991) 254.
[3] M. Geijsberts et al., Nucl. Instr. and Meth. A 313 (1992) 377.
[4] R. Bouclier et al., Nucl. Instr. and Meth. A 323 (1992) 240.
[5] F. Angelini et al., Proc. ECFA workshop for LHC, Aachen 1990, CERN 90-10, vol III, p. 222.
[6] F. Udo, Proc. ECFA workshop for LHC, Aachen 1990, CERN 90-10, vol III, p. 219.
[7] ATLAS Letter of Intent, CERN/LHCC 92-4, October 1992.
[8] CMS, The Compact Muon Solenoid. Letter of Intent, CERN/LHCC 92-3, 1 October 1992.
[9] S. Margetides, CMS collaboration, private communication.
[10] J. Schmitz, Nucl. Instr. and Meth. A323 (1992) 638;
J. Schmitz, preprint NIKHEF-H/93-07, submitted to the Proc. of the MC93 conference, Tallahassee, ed. Dragovitsch (World Scientific, 1994) p. 293.
[11] Desag D263 glass. The photolithography was done by SRON, Utrecht.
[12] Manufactured by RAL Rutherford.
[13] Manufactured by CERN.